



## REVISITING HELIX CLASSIFIERS

José Aurélio Medeiros da Luz <sup>1</sup>

<sup>1</sup> School of Mines at Federal University of Ouro Preto –UFOP.Campus Universitário, Bauxita, 35400-000 Ouro Preto MG, Brazil.

### ABSTRACT

*Helix classifier is a classic equipment in ore dressing. The aim of this study was to provide engineering students and process engineers with a new method to sizing simplex, duplex and triplex helix classifiers. It was developed from particuology, fluid dynamics and literature data. New formulae for classifier calculation and sizing were accomplished. The resulting construct allows the straightforward development of computer software in order to size this equipment, with only the fluid density and viscosity and basic properties of the granular system being processed as input.*

**Keywords:** Size Separation, Spiral, Settling.

### INTRODUCTION

Splitting in mineral processing unit operations can be grouped into two main classes: sizing (size separation) and sorting (species separation, or concentration). In size separation, at least two distinct products are generated: one coarser (oversize) and the other finer (undersize) than the feed. Among size separation equipment used in the industry currently, stand out: screens, sedimentation chambers; countercurrent or vertical hydraulic classifiers; mechanical classifiers; centrifugal classifiers (hydrocyclones and pneumatic cyclones).

Helix classifiers (commonly and improperly referred to as spiral classifiers) are part of so-called mechanical classifiers, because they have a mechanism to remove settled solids. (Figure1).

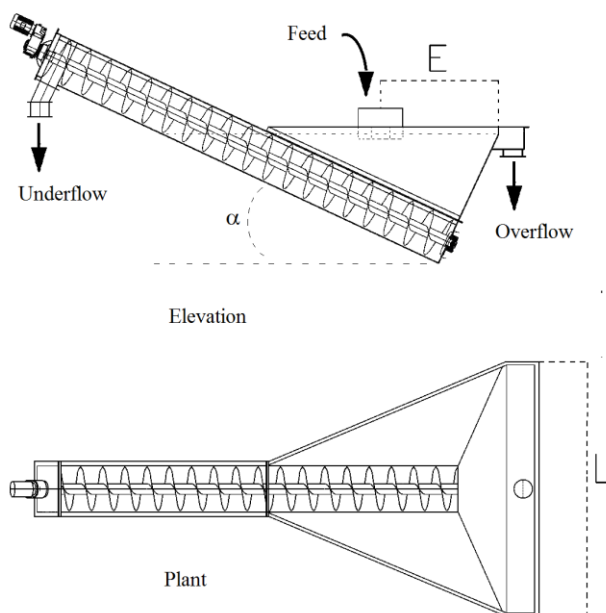


**Figure1 – Helix classifier scheme.**

Helix classifiers are specified by the nominal diameter of their screw conveyor. The manufacturers usually produce equipment with 100 %, 125 % and 150 % submergence of the helix at the lower end, immersed in the basin (Reed, 2002). The larger the submergence, the finer the particle size cut, because of the greater deposition basin area.

The application of the mechanical classifiers was greatly reduced with the advent of hydrocyclones (first patent in 1891), since hydrocyclones handle higher slurry flow rates, with finer cut size, and with much less physical area requirements in the plant, although more prone to operation instability. Nowadays, only hydrocyclones are practically applied for the closing of grinding circuits.

Thus, the application of mechanical classifiers ended up occupying a specific niche, usually when it comes to small flow rates and coarser cut sizes. They have, however, the advantage of allowing better dewatering of the coarse product (underflow) and less fine entrainment in that stream (even accepting, washing by sprinkling on surfaced parts of the underflow trough).

A successful example of helix classifier's modern use is in sizing operation of sinter feed (between 0.15 mm and 6.0 mm) in iron ore and manganese ore processing routes, since, unlike hydrocyclones, this equipment accepts coarse feeds without risk of clogging.

### FLUID DYNAMIC FEATURES

#### Settling velocity of isolated spherules

Rigid particle of diameter  $d_p$ , free-falling in a viscous medium under gravitational field, after an initial stage of decreasing acceleration, develops an equilibrium terminal velocity. In any case, at an arbitrary time, its velocity ( $v$ ) depends on the density difference, its shape and the so-called Reynolds number ( $Re = \frac{\rho_f \times v \times d_p}{\mu}$  where  $\rho_f$  is the fluid density and  $\mu$  is the fluid dynamic viscosity).

The Reynolds number represents the ratio, less than a constant, between the inertial and viscous forces involved

in the system. The numerical limits between the laminar, intermediate and turbulent ranges are not very well defined. The following limits are generally and somewhat arbitrarily adopted:  $Re < 0.2$  for laminar flow;  $0.2 < Re < 1,000$  for intermediate or transitional flow;  $Re > 1,000$  for turbulent flow.

A particle immersed and moving in viscous fluid within a uniform gravitational field (or, mutati mutandis, a centrifugal field) is subject to the following forces: weight, Archimedean thrust and the fluid resistance force, referred to as drag. The resultant force therefore is:  $F = P - E - F_d$ , where  $P$  is the weight,  $E$  the thrust and  $F_d$  the drag force, dependent on velocity,  $v$ .

The drag force, for the usual range of  $Re$ , is monotonically increasing with speed. Generally can be expressed by:

$$F_d = \frac{1}{2} \times \rho_f \times v^2 \times A_p \times C_d \quad (01)$$

Where  $A_p$  is the cross-sectional area of the particle. The structure of the dimensionless drag coefficient ( $C_d$ ) consists of two intrinsic components: a geometric one, which would allow to quantify the real surface of the particle's front edge; and another component, which is linked to dissipative fluid dynamic effects associated with friction and the downstream wake's eddies, which are dependent on the level of turbulence (in other words, dependent on the Reynolds number).

Asymptotic (terminal) velocity occurs when drag equals particle's apparent weight. For a sphere, equating the fluid-dynamic resistance to the apparent weight and taking the expressions for cross-sectional area and volume, the terminal velocity can be calculated by:

$$v_t(d_p, c_v = 0) = \sqrt{\frac{4}{3} \times \frac{(\rho_s - \rho_f) \times d_p \times g}{\rho_f \times C_d}} \quad (02)$$

The drag coefficient is  $Cd = 24/Re$  in the laminar range ( $Re < 0.2$ ). In Newton's range ( $1,000 < Re < 200,000$ ):  $Cd = 0.44$ . In the transitional or intermediate regime (which is more common in the ore dressing operations, i.e.:  $0.2 < Re < 1,000$ ), the drag coefficient must be achieved iteratively.

Many empirical and semi-empirical equations have been proposed for the intermediate or transitional flow regime (Almendra, 1979, Clezar and Nogueira, 1999, King, 2001, Tosun, 2002, Massarani, 2002 and Kroetz, 2013; De Felice, 2007). An equation with excellent adherence is that from Turton-Levenspiel:

$$C_d = \frac{24}{Re} \times (1 + 0.173 \times Re^{0.657}) + \frac{0.413}{1 + 16,300 \times Re^{-1.09}} \quad (03)$$

The present author has gotten the following equation:

$$C_d = \frac{22.717}{Re^{1.0325}} + 2.4414 \times \left\{ 1 - \exp[-17.0330 \times Re^{-0.9975}] \right\} + 0.44$$

(04)

As force is mass times acceleration, and velocity is the derivative of acceleration, after some arrangements and integration in the laminar regime, for an arbitrary time  $t$  (with  $t_0 = 0$  s), one attains to the following equation for settling velocity:

$$v = \left\{ v_0 + \left[ \frac{1}{18 \times \eta} \times (\rho_p - \rho_f) \times g \times d_p^2 \right] \right\} \times \exp \left[ -\frac{18 \times \eta}{\rho_p \times d_p^2} \times t \right] - \frac{1}{18 \times \eta} \times (\rho_p - \rho_f) \times g \times d_p^2 \quad (05)$$

It should be noted that velocity tends to the Stokes equation when time tends to infinity. Remembering the instantaneous velocity is the derivative of the distance traveled, it can be attained from integration of the preceding equation.

### Settling velocity of particles in slurry

The movement of non-isolated particles (with volumetric concentration,  $c_v$ ) is perturbed by the interaction between their streamlines, resulting in certain interstitial turbulence, which leads to the deviation in the previous equations, being necessary the application of a multiplicative correction coefficient ( $f(c_v)$ ). This correction function can be expressed by an equation available in the literature, such as that of Steinour, van Rijn, Merkel. We mention here that one from da Luz (2005):

$$f(c_v) = \left( 1 - c_v^{0.919} \right)^{4.681} \quad (06)$$

### Settling velocity of non-spherical particles

The equations for non-spherical particles must be affected by another multiplicative shapecorrection ( $f(\psi)$ ), which has not been rigorously quantified to date. Corrections usually employed are based on Wadell's sphericity ( $\psi$ ), such as those due to Pettyjohn and Christiansen (Almendra, 1979; Geldart, 1990).

- In Stokes' range:

$$f(\psi)_s = 0.843 \times \log_{10} \left( \frac{\psi}{0.065} \right) \quad (07)$$

- In Newton's range:

$$f(\psi)_N = \sqrt{\frac{0.43}{5.31 - 4.88 \times \psi}} \quad (08)$$

It should be noted that, for the transitional or intermediate regime, in the absence of a specific equation, one can adopt the linear interpolation proposed by Geldart (Geldart, 1990; Arsenijevic et al., 1999).

With a high volumetric concentration of particles, there is

the zone sedimentation regime. Treatment of experimental cloud of points from numerous tests (Luz, 2009) allowed the establishment of the following equation describing the evolution of the height ( $z$ ) of the interface between the clarified liquid and the slurry blanket in graduated cylinders:

$$z(t) = (z_0 - z_\infty) \times \left( 1 - \frac{t^a}{t^a + b^a} \right) + z_\infty \quad (09)$$

Where:

$z_0$  – height of the clarified interface at time  $t$  [s];

$z_\infty$  – equilibrium height of the clarified interface at time  $t = \infty$  [s].

$a$  and  $b$  – parameters of the model, which depend on the particles properties and the physical-chemical environment.

The parameter  $a$  is dimensionless, while  $b$  represents the time for sedimentation height to reach 50 % of its final course (similar to the concept of half-life in physics and chemistry).

The above equation has been validated with numerous tests with many materials, such as iron ores, manganese ore, aluminum hydroxide, clays from hydrocyclones overflow from gravity processing plants. The zone settling velocity is attained by its derivative with respect to rest time, providing the following expression:

$$v(t) = \frac{dz(t)}{dt} = -(z_0 - z_\infty) \times \left[ \frac{a \times b^a \times t^{a-1}}{(t^a + b^a)^2} \right] \quad (10)$$

## HELIX CLASSIFIER SIZING

### Required power

The power consumed by a helix classifier depends on its size, the density of the processed material and the angular velocity of its screw conveyor. Literature data are scarce. However, from regression analysis of data tabulated by Rabone (1957), the so-called specific effective power can be expressed by:

$$P_{esp} = 416 \times \varphi^{2.923} + 125 = \frac{P}{N} \quad (11)$$

Where:

$P_{esp}$  – specific power [W/rpm];

$\varphi$  – diameter of screw (helix) [m].

The nominal power ( $P_n$ ), expressed in watts, can be

calculated from the equation given by:

$$P_n = 2 \times P_{esp} \times N \quad (12)$$

Where:  $N$  – angular velocity of screw conveyor [rpm].

In turn, the angular velocity must ensure sediment reclaim, without causing turbulence in the classifier's sedimentation basin, which tends to resuspend solids and to cause entrainment of unwanted coarse particles into the overflow stream.

$$N_{max} = 20.88 \times \exp(-1.148 \times \phi) + 3.73 \quad (13)$$

The slope of the classifier axis will ultimately affect the settling basin area, and therefore the operation's cut size. In general, the slope angle falls between 15° and 20°.

### Sizing procedure from basin area

Most texts in the area (Beraldo, 1987; Galery, 2007; Wills and Napier-Munn, 2006) size mechanical classifiers as mere hydraulic classifiers. The settling velocity of cut size particles is matched to the ascending mean velocity of the overflow slurry. Such latter velocity is attained by dividing the overflow's upward volumetric flow rate of overflow by the pool area.

The continuity equation allows us to set these equations:

$$Q_{vo} = \frac{Q_{vs_o}}{c_{vo}} = \frac{\rho_s}{c_{vo}} = \frac{Q_{s_o}}{c_{vo} \times \rho_s} = v_t(d^*, c_{vo}, \psi) \times A_t \quad (14)$$

(14)

Where:

$Q_{vo}$  – volumetric flow rate of overflow slurry (solid plus fluid) [m<sup>3</sup>/s];

$Q_{vs_o}$  – volumetric flow rate of solids in overflow [m<sup>3</sup>/s];

$Q_{s_o}$  – mass flow rate of solids in overflow [kg/s];

$c_{vo}$  – volumetric concentration of solids in overflow [-];

$d^*$  – nominal cut size [m];

$v_t$  – terminal settling velocity of cut size particles (as function of  $d^*$ ,  $c_{vo}$  and  $\psi$ ) [m/s];

$\rho_s$  – particle density (solid) [kg/m<sup>3</sup>];

$A_t$  – effective transverse cross-sectional area of upward hydraulic flow tube of overflow [m<sup>2</sup>].

Rearranging the previous equation, considering as effective area:  $A_t = L \times E$  and affecting it of an empirical coefficient  $k_{cla}$ , one has for solid mass flow rate at overflow:

$$Q_{s_o} = k_{cla} \times L \times E \times c_{vo} \times \rho_s \times v_t(d^*, c_{vo}, \psi)$$

(15)

Where:

**E** – classifier’s weir width (see Figure 1)[m];

**L** – distance between feed box and weir (see Figure 1) [m].

The empirical parameter ( $k_{cla}$ ) takes into account not only the fact that the effective cross-sectional area is not equal to  $B \times L$ , but also because there is some turbulence caused by the helix rotation during the continuous removal of the underflow. However most texts do not even mention  $k_{cla}$  (implicitly adopting unit value for this parameter).

In this regard, Gaudin (1975) has criticized the use of  $k_{cla} = 1.0$ , stating that the performance of these equipment was substantially lower than that given by the equation considering such a value, without, however, presenting an alternative for its estimation (other than the alternative of consulting the manufacturers' catalogs). On the other hand, Fitch and Roberts (1985) give the range:  $0.2 < k_{cla} < 0.6$ .

With regard to the terminal velocity, it can be determined from Equations 02, 04 (or 03), 06, 07 and 08 (iteratively if in transitional range of  $Re$ ).

**Sizing procedure from Razumov and coworkers' data**

A more elaborate method for sizing helix classifiers is that table-based procedure presented by Razumov and Perov (1985). These authors have presented several tables for correction of their basic formulas, in order to meet process conditions, such as slope of the classifier axis, the fineness of the cut, the slurry dilution and the density of the processed solid material. According to these authors the processing capacities for underflow and overflow streams are given by:

- Solid mass flow rate in overflow stream (in kg/s):

$$Q_{s\_o} = 4.681 \times 10^{-4} \times n_h \times \rho_s \times k_\alpha \times k_\beta \times k_\gamma \times \phi^{1.765} \quad \text{[kg/s]} \quad (16)$$

- Solid mass flow rate in underflow stream (in metric kg/s):

$$Q_{s\_u} = 5.607 \times 10^{-4} \times \rho_s \times n_h \times N \times k_\alpha \times \phi^3 \quad \text{[kg/s]} \quad (17)$$

The exponent of the overflow equation is compatible with corresponding value obtainable by the Taggart's data (Taggart, 1945), which is equal to 1.768 for H-type (“high weir”) classifier and 1.831 for S-type (“submerged helix”) classifier.

In addition the nomenclature already used, in the two equations above, we have:

$n_h$  – numbers of helices [-];

$N$  – angular velocity of the helix [rpm];

$k_\alpha$ – correction coefficient due to classifier's slope [-];

$k_\beta$ – correction coefficient due to the fineness of the solids in the overflow [-];

$k_\gamma$ – correction coefficient due to dilution in overflow [-];

The original correction coefficients are tabulated in Razumov et al. (1985). These parameters can, however, be obtained by using the following equations, developed for the present work, in order to allow the easy implementation of a computational system for helix classifier sizing.

$$k_\alpha = 1.54 - 0.031 \times \alpha \quad (18)$$

$$k_\beta = 2.5 \times [1 - \exp(-3,580 \times d_{95})] \quad (19)$$

Where:

$d_{95}$  – maximum nominal diameter of particles in overflow [m];

$\alpha$  – slope angle of the classifier [°].

The correction due to the overflow dilution, from the Razumov and Perov's data (Razumov and Perov, 1985), can be expressed by the nonlinear regression equation:

$$k_\gamma = 1.28 \times 10^{-5} \times \rho_s + 1.72 \times 10^{-7} \times \left(\frac{D_o}{D_{ref}}\right)^{38.532} + 2.376 \times 10^{-4} \times \rho_s \times \left(\frac{D_o}{D_{ref}}\right)^{1.058} + 0.3193 \quad (20)$$

Where:

$D_o$ – dilution of classifier overflow [-];

$D_{ref}$ – reference (basic) dilution of classifier overflow [-];

The previous equation gives very good statistical adherence to the tabulated data (Figure 3) with a mean modulus of the relative error of 0.3 % (and with modulus of maximum relative error of 1.0 %).

Dilution ( $D$ ) is the ratio of fluid mass (liquid) to mass of solids in the slurry. Thus, the mass concentration of solids ( $c_m$ ) and the dilution are interrelated as follows.

$$D = \left(\frac{1 - c_m}{c_m}\right) \quad (21)$$

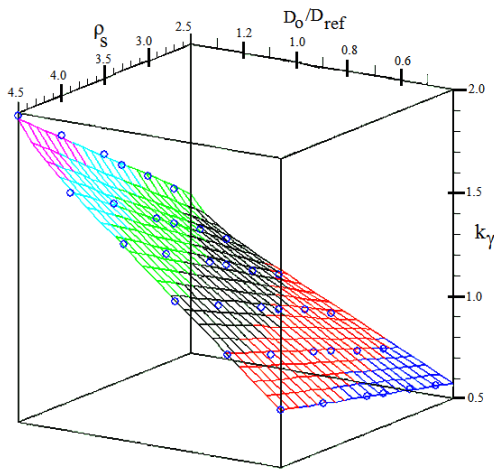


Figure 2 -Regression surface from Razumov and Perov's data (circles).

In turn, the volumetric solids concentration and the dilution are related by the following expression:

$$c_v = \left( \frac{V_s}{V_s + V_f} \right) = \left( \frac{\frac{m_s}{\rho_s}}{\left( \frac{m_s}{\rho_s} + \frac{m_f}{\rho_f} \right)} \right) = \left( \frac{m_s}{m_s + m_f} \right) \times \frac{\rho_p}{\rho_s} = c_m \times \frac{\rho_p}{\rho_s} = \left( \frac{1}{1 + D} \right) \times \frac{\rho_p}{\rho_s} \quad (22)$$

Letters *m*, *V* and  $\rho$  stand for mass, volume and density, respectively, whereas subscripts *f*, *p* and *s*, for fluid (liquid), pulp (slurry) and solid, respectively.

For its part, the reference dilution (or basic dilution) is the one normally used for the classifying operation, which is dependent on the desired cut size; ultimately, on the particle size of the solids in the overflow. It can be expressed, with good precision, by:

$$D_{ref} = \frac{4.1567 \times 10^{-5}}{d_{95}^{1.22}} + 1.2 \quad (23)$$

With the maximum nominal particle diameter at overflow (*d*<sub>95</sub>) expressed in meters.

A mass balance allows the calculation of the dilution at the overflow, using the solid mass flow rate in the feed (*Q*<sub>*s*,*f*</sub>) and in the underflow, besides the solid mass concentrations of these two streams (*c*<sub>*m*,*f*</sub> at feed and *c*<sub>*m*,*u*</sub> at underflow). The fluid flow rates (water) in the feed and underflow are:

$$Q_{fl_f} = \frac{Q_{s_f}}{c_{mf}} - Q_{s_u} = Q_{s_f} \times \left( \frac{1}{c_{mf}} - 1 \right) \quad (24)$$

$$Q_{fl_u} = \frac{Q_{s_u}}{c_{mu}} - Q_{s_u} = Q_{s_u} \times \left( \frac{1}{c_{mu}} - 1 \right) = R_s \times Q_{s_f} \times \left( \frac{1}{c_{mu}} - 1 \right) \quad (25)$$

The difference between the inlet water and underflow water is the overflow water. In turn, the mass flow rate of solids at the overflow, for given underflow solid recovery (*R*<sub>*s*</sub>) can be expressed by:

$$Q_{s_o} = Q_{s_f} - R_s \times Q_{s_f} = Q_{s_f} \times (1 - R_s) \quad (26)$$

The expression for the dilution is finally:

$$D_o = \frac{Q_{f-f} - Q_{f-u}}{Q_{s_o}} = \frac{\left( \frac{1}{c_{mf}} - 1 \right) - R_s \times \left( \frac{1}{c_{mu}} - 1 \right)}{1 - R_s} \quad (27)$$

As the required solids flow rate is constant, when the dilution of the feed slurry is varied there will be a change in the volumetric flow rate of the slurry and, therefore, in the classifier's cut diameter. The amount of particle size change in the products caused by dilution ultimately depends on the current fluid dynamics regimen (if laminar or turbulent conditions exist). Consequently, the equation of continuity (Equation 14) and the previous fluid dynamic equations allow calculating the classifier's cut size:

- Laminar or Stokes' range:

$$d_p^* = \sqrt{\frac{18 \times \eta \times Q_{s_o}}{g \times \rho_s \times (\rho_s - \rho_f) \times c_v \times (1 - c_v^{0.919})^{4.861} \times A_t}} \quad (28)$$

- Turbulent or Newton's range:

$$d_p^* = \frac{0.33 \times Q_{s_o}^2 \times \rho_f}{g \times \rho_s^2 \times (\rho_s - \rho_f) \times c_v^2 \times (1 - c_v^{0.919})^{9.722} \times A_t^2} \quad (29)$$

Using non-linear regression on Shoemaker's data (Shoemaker, 1989), the dynamic viscosity of liquid water (in Pa.s), as a function of temperature (*T*, in kelvins), can be calculated by:

$$\eta_{H_2O} = 0.00156 \times \exp \left[ -0.044887 \times (T - 273.15)^{0.91568} \right] + 0.00023 \quad (30)$$

The dilution where the minimum cut size occurs is called critical dilution. It is seen that in the Stokes' range the critical dilution is that one for which the volumetric fraction is about 12 %, whereas, in the Newton's range,

around 16 %. For transitional fluid dynamic regime, the critical values are intermediate to those of cited extremes.

An interesting aspect of the Razumov and Perov equation (Equation 16) is that it allows the scaling up, attaining, in an immediate way, the dimensions of an industrial scale classifier, having done only laboratory tests. By adopting the subscript "ind" for industrial scale and "lab" for laboratory scale, the diameter of the industrial classifier can be calculated by:

$$\phi_{ind} = \left[ \frac{Q_{s\_o\_lab}}{Q_{s\_o\_ind} \times \phi_{lab}^{1.765}} \times \frac{n_{hind} \times k_{\alpha ind} \times k_{\beta ind} \times k_{\gamma ind}}{n_{hlab} \times k_{\alpha lab} \times k_{\beta lab} \times k_{\gamma lab}} \right]^{1/0.765} \quad (31)$$

**Partition curve**

The global partition of solids for underflow ( $R_s$ ) is the underflow solids mass rate divided by the solids mass flow rate in the feed. The partition by size class is the analogous concept, taking each granulometric class ( $i$ ) individually:  $Y_i = Y(x_i) = Q_{s\_u}(i)/Q_{s\_f}(i)$ , which is called partition curve. It allows the diagnosis of the classification process. The actual partition curve,  $Y(x_i = 0) > 0$ . The equipartition diameter, that is: the particle diameter for which 50 % of this class report to underflow, is referred to as  $d_{50}$ .

The fluid in the underflow carries part of the particles, not through the effective size partition mechanisms of the classifier. This phenomenon is general for all sorts of classifiers and is called bypass or short-circuit.

As a matter of fact, a much smaller proportion of the coarse material can erroneously be reported to the overflow, by mechanical entrainment or drag. It is the coarse fraction short-circuit, but usually it is negligible.

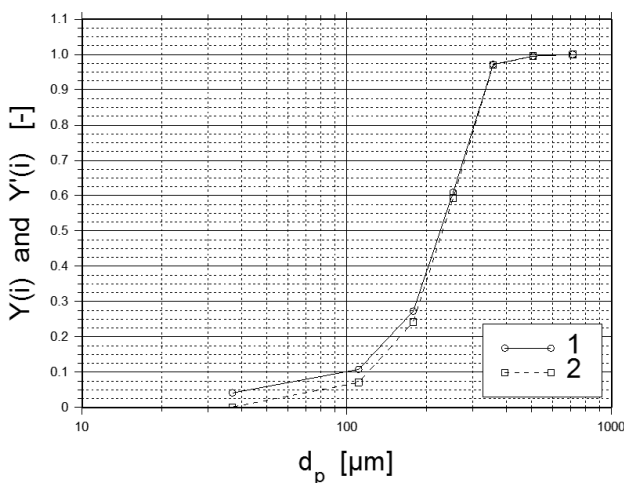


**Figure3 – Typical helix classifier partition curve. Curve 1:  $Y(i)$  – actual partition; curve 2:  $Y'(i)$  – purged partition (without bypass using Kelsall's criterion).**

Thus, the purged partition curve plotting these erroneously reported parcels is called improperly "corrected" partition curve. In fact, this curve is important only in mathematical modeling of this process and can be seen in several textbooks, such as Wills and Napier-Munn (2006), Gupta and Yan (2006), Kelly and Spostwood (1982). Usually, Kelsall's unprovable criterion is used, whereby all size classes have the same drag percentage that is equal to the fluid partition to the underflow ( $R_f$ ). Using this criterion, one has the following expression of the purged partition in a generic size class:

$$Y'_i = \frac{Q_{s\_u}(i) - R_f \times A_i}{Q_{s\_f}(i) - b p_i} = \frac{Q_{s\_u}(i) - R_f \times A_i}{Q_{s\_f}(i) - R_f \times A_i} = \frac{Q_{s\_u}(i) - R_f \times A_i}{Q_{s\_f}(i) - R_f \times Q_{s\_f}(i)} = \frac{Y_i - R_f}{1 - R_f} \quad (32)$$

Naturally, using this criterion, we will have  $Y'(x_i = 0) = 0$ . In any case, given the grain size distribution of the feed, the solids recovery to the underflow can be calculated by integrating the partition equation for the entire size range. For discrete systems (with  $n_c$  size classes), this recovery is the weighted average of the partition values, with the retained mass fractions ( $f_i$ ) as weights for each size class. That is:

$$R_s = \sum_{i=1}^{n_c} f_i \times Y_i = \sum_{i=1}^{n_c} f_i \times \frac{Q_{s\_u}}{Q_{s\_f}} \quad (33)$$

The purged distribution in general can be mathematically modeled by the Rosin-Rammler-Sperling-Bennett distribution, a special case of the Weibull distribution for  $\delta = 0$  (Plitt, 1976; King, 2001; Mular, 2003; Gupta and Yan, 2006; Luz, 2005):

$$Y = p(0 \leq x \leq X) = 1 - \exp \left[ - \left( \frac{d_p}{d^*} \right)^\beta \right] = 1 - \exp \left[ \ln \left( \frac{1}{2} \right) \times \left( \frac{d_p}{d_{50}} \right)^\beta \right] \quad (34)$$

Where  $\beta$  is the sharpness index and  $d^*$  is the scale parameter of the distribution.

**CONCLUSION**

Currently, helix classifiers occupy specific niche in the treatment of particular systems. Due to the better dewatering of the underflow, the actual partition curve of the helix classifiers presents greater adherence to the theoretical curve, compared to hydrocyclones. Another front in which helix classifier is preferred than hydrocyclones until today is washing and classification of coarse feeds, like iron ore sinter feed.

The equations of the method developed here allow the

straightforward development of computational system for helix classifier sizing and design, based on the basic properties of the fluid and the processed material.

## REFERENCES

1. ALMENDRA, E. R. *Velocidade de Sedimentação de Sistemas Particulados*. Rio de Janeiro: COPPE/UFRJ, 1979. 88 pp.
2. ARSENIJEVIC, Z, Lj. et alii. *Determination of non-spherical particle terminal velocity using particulate expansion data*. *Powder Technology*. Vol. 103, 1999; pp. 265–273.
3. BERALDO, J. L. *Moagem de Minérios em Moinhos Tubulares*. São Paulo: Edgard Blucher, 1987. 143 pp.
4. DI FELICE, R. *Liquid suspensions of single and binary component solid particles—An overview*. *China Particuology*. V. 5 (2007); pp: 312–320.
5. FITCH, B; ROBERTS, E. J. in: Weiss, N. L. (Ed) *SME Mineral Processing Handbook*, AIME, 1985, pp. 3D 1-10.
6. GAUDIN, A. M. *Principles of Mineral Dressing*. New York: Mcgraw – Hill, 1975.
7. GELDART, D. *Estimation of Basic Particle Properties for Use in Fluid-Particle Process Calculations*. *Powder Technology*. Volume 60, n. 1, January 1990, Pages 1-13.
8. GUPTA, A. & YAN, D. S. *Mineral Processing Design and Operations: an Introduction*. Amsterdam: Elsevier, 2006. 718 p.
9. KING, P. *Modeling and Simulation of Mineral Processing Systems*. Boston: Butterworth-Heinemann, 2001. 403 pp.
10. KROETZ, T. *O efeito da “crise do arrasto” no mergulho de altura (The effect of “drag crisis” on plungedive)*. *Revista Brasileira de Ensino de Física*, v. 35, n. 3, 3308 (2013).
11. LUZ, J. A. M. *Aspectos Reológicos de Polpas em Sedimentação*. In: *Congresso Anual da ABM, 2009, Belo Horizonte. Anais do 64o. Congresso da ABM*. São Paulo: ABM, 2009. v. 1. p. 1-11.
12. LUZ, J. A. M. *Conversibilidade entre distribuições probabilísticas usadas em modelos de hidrociclones*. *Revista Escola de Minas, Ouro Preto*, V. 58(1), pp: 89-93, janeiro/março, 2005.
13. MASSARANI, Giulio. *Fluidodinâmica em Sistemas Particulados (2ª ed.)*. Rio de Janeiro: E-papers. 2002. 152 p.
14. MULAR, A. *Size Separation*. In: FUERSTENAU, M. & HAN, K. N. *Principle of Mineral Processing*. Littleton: SME, 2003. Chapter 4, p. 119-172.
15. PLITT, L. R. *A Mathematical Model of the Hydrocyclone Classifier*. *CIM Bulletin*. December, 1976. pp. 114 – 123.
16. RABONE, Ph.. *Flotation Plant Practice (4th ed.)*. London: Mining Publications, 1957. 255 pp.
17. RAZUMOV, K. A. & PEROV, V. A. *Proyectos de Fábricas de Preparación de Minerales*. Moscú: Mir, 1985.
18. REED, W. M. *Sizing and Application of Gravity Classifiers*. In: Mular, A. et. Alii (ed.). *Mineral Processing Plant – a Design, Practice, and Control Proceedings*. Littleton: SME, 2002.
19. SHOEMAKER, D. P. et alii. *Experiments in Physical Chemistry*. McGraw-Hill. New York, 1989.
20. WILLS, B.; NAPIER-MUNN, T. J. *Will's Mineral Processing Technology (7th ed.)*. Burlington: Butterworth-Heinemann, 2006.